

Optimization and Prediction in Natural Gas Networks Using Graph Neural Networks and MPCC-Based Models

Author: Cristian Alejandro Blanco Martínez

Director: David Augusto Cárdenas Peña

Universidad Tecnológica de Pereira
Grupo de investigación Automática

September 24, 2025



Agenda

- 1 Motivation & Problem Statement
- 2 Objectives
- 3 Natural Gas System Prediction Using Graph Neural Networks
- 4 Natural Gas System Optimization Using MPCC-Based Models
- 5 Physics-Guided Neural Networks for Gas Networks under Uncertainty
- 6 Conclusions and Future Work
- 7 Bibliography

Energy Context & Relevance of Natural Gas

In Colombia, natural gas is widely used across the residential, commercial, industrial, and thermal power sectors. Its importance becomes evident during dry seasons, when hydroelectric generation is reduced and thermal plants, fueled by natural gas, step in to maintain electricity supply [Promigas, 2021].



Motivation & Problem Statement

- **Large-scale natural gas networks** require solving complex optimization problems [Sharifi et al., 2022].
- Increasing network size and operational constraints lead to:
 - Long execution times
 - Difficulty in real-time or near real-time decision making
- Classical approaches are accurate but often **computationally expensive**.

Solving a network with 592 nodes and 460 edges takes 5 min on average, while a larger one with 660 nodes and more than 500 edges requires 30 min using the same MILP-based optimizer [Pfetsch et al., 2014].

Main Problem: There is a need for methods that preserve accuracy while significantly reducing computation time.

Problem Statement: Specific Challenges

From the general problem of natural gas transportation optimization, three specific challenges can be identified:

- ① **High computational cost:** Solving large-scale optimization problems requires long execution times, limiting the feasibility of real-time or near real-time operation.
- ② **Pipeline modeling complexity:** The Weymouth equation introduces nonlinearities, discontinuities, and nonconvexities that generate approximation errors and numerical instability.
- ③ **Uncertainty in demand:** Variability in hydropower generation and the growth of renewable sources create uncertainty in the demand for natural gas, requiring flexible and stochastic optimization approaches.

Research Question: How can an optimization tool be developed that seeks to improve the solution to the problem of natural gas transportation, taking into account computational cost, growing energy demand, and the uncertainty associated with this factor?

Objectives

General Objective:

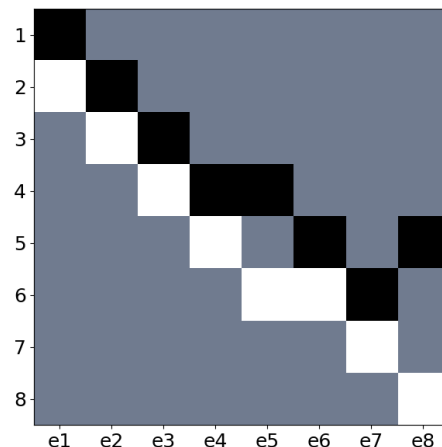
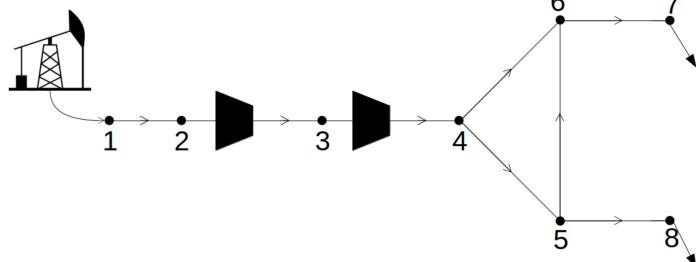
- Develop an optimization tool that integrates knowledge of the gas transportation network topology, a suitable approximation of the Weymouth equation and stochastic optimization techniques to address the gas transportation task taking into account the uncertainties related to hydroelectric generation and the growth of alternative energy sources.

Specific Objectives:

- ① Design a Graph Neural Networks-based approach of regression that integrates knowledge of natural gas network topology to reduce computational time for operation estimation.
- ② Develop an optimization model for natural gas transportation systems that takes into account the Weymouth equation for reducing that reduces the approximation error in pipeline gas flow calculations.
- ③ Develop a stochastic gas flow dispatch optimization strategy that quantifies the uncertainty in the objective variables and decision variables associated with the operation of the gas system taking into account the constraints of the transportation problem.

Objective 1 - Natural Gas System as a Graph

A natural gas network can be represented as a directed graph, where nodes correspond to elements such as wells, users, or storage facilities, and edges represent pipelines and compressors.



Objective: Achieve near-optimizer accuracy with significant runtime reduction.

Optimization Problem: Objective and Constraints

The gas network consists of wells \mathcal{W} (supply nodes), pipelines \mathcal{P} , compressors \mathcal{C} and unsupplied demand \mathcal{U} (demand nodes)

$$\min_{\mathcal{P}, \mathcal{F}} \sum_{t \in \mathcal{T}} \left(\sum_{w \in \mathcal{W}} C_w f_w + \sum_{p \in \mathcal{P}} C_p f_p + \sum_{c \in \mathcal{C}} C_c f_c + \sum_{u \in \mathcal{U}} C_u f_u \right)$$

where C_i is the cost per unit flow at element i , and f_i is the corresponding gas flow.

$$\underline{f}_w \leq f_w \leq \overline{f}_w \quad \forall w \in \mathcal{W} \quad \text{Well capacity} \tag{1}$$

$$-\overline{f}_p \leq f_p \leq \overline{f}_p \quad \forall p \in \mathcal{P} \quad \text{Pipeline limits} \tag{2}$$

$$0 \leq f_u \leq \overline{f}_u \quad \forall u \in \mathcal{U} \quad \text{Demand satisfaction} \tag{3}$$

$$\sum_{m: (m, n) \in \mathcal{A}} f_m = \sum_{m': (n, m') \in \mathcal{A}} f_{m'} \quad \text{Nodal gas balance} \tag{4}$$

CensNet Layers: Integrating Node & Edge Features

Motivation: Traditional GCNs focus mainly on *node features* and ignore *edge features*, missing part of the graph's information.

CensNet innovation:

- Alternates between **node layers** and **edge layers**.
- Each layer type updates its own features while using information from the other:
 - **Node layer:** Node embeddings are updated using both node adjacency and transformed edge features.
 - **Edge layer:** Edge embeddings are updated using edge adjacency and transformed node features.
- Uses an *incidence matrix* \mathbf{T} to switch between node and edge domains.

Benefits:

- Captures both *structural* (adjacency) and *relational* (edge) information.
- Enhances long-range dependencies through alternating propagation.

Node layer propagation

$$\mathbf{H}_v^{(l+1)} = \sigma \left((\mathbf{T} \Phi(\mathbf{H}_e^{(l)} \mathbf{p}_e) \mathbf{T}^\top \odot \tilde{\mathbf{A}}_v) (\mathbf{H}_v^{(l)} \mathbf{W}_v) \right)$$

Definitions:

- N_v : number of nodes.
- D_v, D'_v : input and output node feature dimensions.
- $\mathbf{H}_v^{(l)} \in \mathbb{R}^{N_v \times D_v}$: node features at layer l .
- $\mathbf{H}_e^{(l)} \in \mathbb{R}^{N_e \times D_e}$: edge features at layer l .
- $\mathbf{p}_e \in \mathbb{R}^{D_e}$: learnable projection vector for edges.
- $\mathbf{T} \in \{0, 1\}^{N_v \times N_e}$: incidence matrix.
- $\tilde{\mathbf{A}}_v \in \mathbb{R}^{N_v \times N_v}$: normalized node adjacency.
- $\mathbf{W}_v \in \mathbb{R}^{D_v \times D'_v}$: learnable weight matrix.
- $\sigma(\cdot)$: non-linear activation, applied element-wise.
- $\Phi(\cdot)$: diagonalization operator.

Edge layer propagation

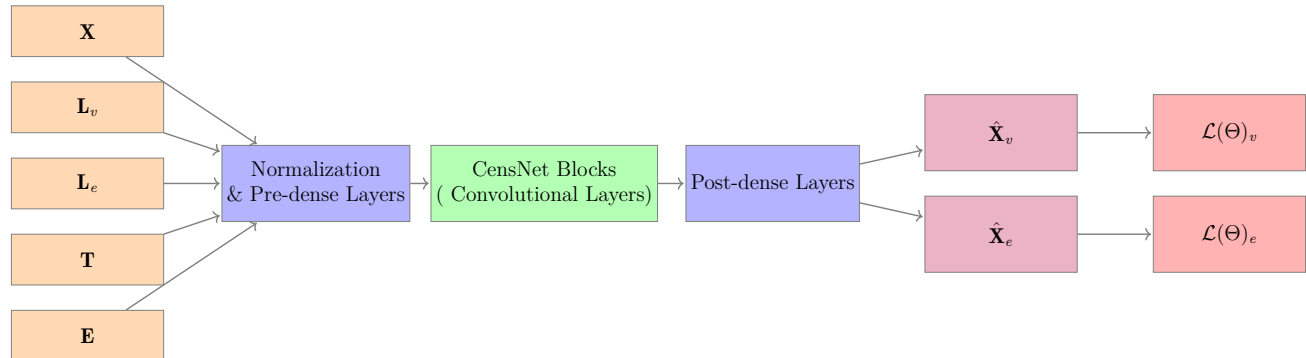
$$\mathbf{H}_e^{(l+1)} = \sigma \left((\mathbf{T}^\top \Phi(\mathbf{H}_v^{(l)} \mathbf{p}_v) \mathbf{T} \odot \tilde{\mathbf{A}}_e) (\mathbf{H}_e^{(l)} \mathbf{W}_e) \right)$$

Definitions:

- N_e : number of edges.
- D_e, D'_e : input and output edge feature dimensions.
- $\mathbf{H}_e^{(l)} \in \mathbb{R}^{N_e \times D_e}$: edge features at layer l .
- $\mathbf{H}_v^{(l)} \in \mathbb{R}^{N_v \times D_v}$: node features at layer l .
- $\mathbf{p}_v \in \mathbb{R}^{D_v}$: learnable projection vector for nodes.
- $\tilde{\mathbf{A}}_e \in \mathbb{R}^{N_e \times N_e}$: normalized edge adjacency (line graph).
- $\mathbf{W}_e \in \mathbb{R}^{D_e \times D'_e}$: learnable weight matrix.
- $\sigma(\cdot)$: non-linear activation, applied element-wise.

Core idea: Information “switches” between node and edge spaces at each step, enriching representations.

CensNet-based Model Architecture



Inputs: Encapsulate both physical attributes and topological information of the network:

- Node features: $\mathbf{X} \in \mathbb{R}^{N_v \times 3}$, injection limits and demand.
- Node Laplacian: $\mathbf{L}_v \in \mathbb{R}^{N_v \times N_v}$, node connectivity.
- Edge Laplacian: $\mathbf{L}_e \in \mathbb{R}^{N_e \times N_e}$, edge connectivity.
- Edge features: $\mathbf{E} \in \mathbb{R}^{N_e \times 5}$, K , β , flow limits.

$$\mathcal{L}(\Theta) = \sum_{r=1}^R \| Y_r - \hat{Y}_r \|_2^2$$

Dataset and Experimental Setup

Two different gas network configurations were used to evaluate the proposed CensNet-based model.

Case	Nodes	Pipes	Comps.	Users
8-node	8	6	2	2
Colombia	63	48	14	27

Different scenarios were generated by adding 5%–25% noise to user demands and solving with APOPT. These outputs were used as training targets for the CensNet model.

Experimental Setup

- **Samples:** 2000 (8-node), 2400 (63-node)
- **Data split:** 60% train, 20% val, 20% test

- **Training:** 1500 epochs, Adam optimizer, Leaky ReLU ($\alpha = 0.2$)
- **Learning rate:** 1×10^{-2} , exponential decay (0.9 every 1000 steps)
- **Hyperparameters:**
 - N_{channels} : 16–64
 - N_{layers} : 1–5 (conv)
 - N_{dense} : 2–32 (post-dense)
- **Losses tested:**
 - Nodal loss only
 - Nodal + edge loss

Performance Comparison: 8-Node and 63-Node Networks

Model	Nodal R^2	Edge R^2	Balance Error	Time (s)
8-node Network				
CensNet (N)	0.988	-2.818	5.71 ± 16.86	0.650 ± 0.442
CensNet (N+E)	0.988	0.999	0.08 ± 1.17	0.640 ± 0.444
63-node Network				
CensNet (N)	0.996	-5.880	0.04 ± 60.83	4.88 ± 5.59
CensNet (N+E)	0.996	0.996	0.01 ± 23.4	4.87 ± 5.59

Prediction speed: T-tests confirm **CensNet is significantly faster** than APOPT

- 8-node: $T = 14.94$, $p = 1.32 \times 10^{-34}$
- 63-node: $T = 47.29$, $p = 4.92 \times 10^{-110}$

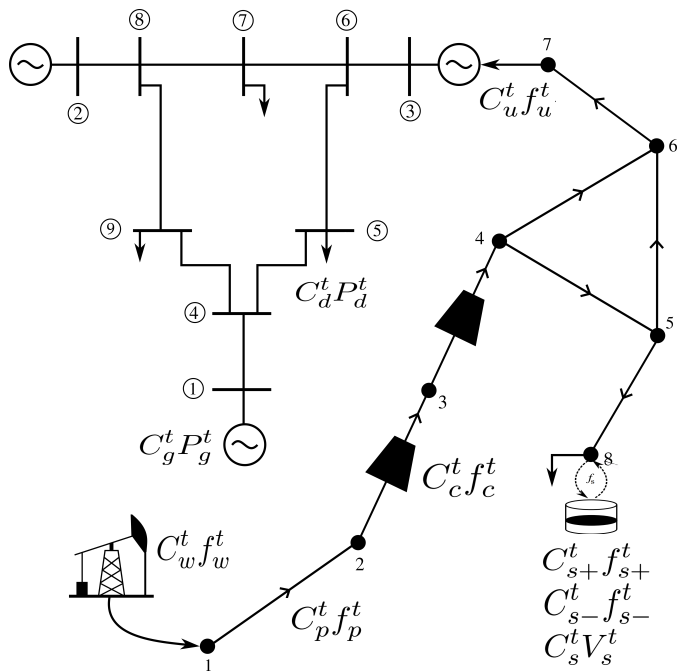
Performance Comparison: 8-Node and 63-Node Networks

Model	Nodal R^2	Edge R^2	Balance Error	Time (s)	T-test
8-node Network					
CensNet (N)	0.99	-2.82	5.7 ± 16.86	0.65 ± 0.4	$T = 15$
CensNet (N+E)	0.99	0.99	0.08 ± 1.17	0.64 ± 0.4	$p = 1.3 \times 10^{-34}$
63-node Network					
CensNet (N)	0.99	-5.88	0.04 ± 60.83	4.9 ± 5.6	$T = 47$
CensNet (N+E)	0.99	0.99	0.01 ± 23.4	4.9 ± 5.6	$p = 4.9 \times 10^{-110}$

The CensNet-based model captures the network's topological information, enabling it to satisfy the gas balance constraint naturally to some extent. Time tests, performed on a single case, confirm that CensNet is significantly faster than APOPT; moreover, being a network-based model, it can efficiently propagate entire batches of scenarios forward.

Interconnected system - Definition

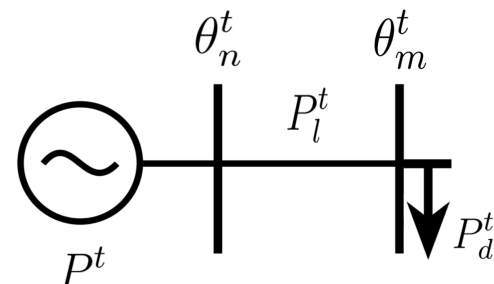
A power-gas interconnected system is a hybrid infrastructure that integrates natural gas and power networks, enhancing overall system efficiency [Duan et al., 2022].



$$\begin{aligned} \min_{\mathcal{P}, \mathcal{F}} \quad & \sum_{g \in \mathcal{G}} C_g^t P_g^t + \sum_{d \in \mathcal{D}} C_d^t P_d^t + \\ & \sum_{w \in \mathcal{W}} C_w^t f_w^t + \sum_{p \in \mathcal{P}} C_p^t f_p^t + \\ & \sum_{c \in \mathcal{C}} C_c^t f_c^t + \sum_{u \in \mathcal{U}} C_u^t f_u^t + \quad (5) \\ & \sum_{s \in \mathcal{S}} C_{s+}^t f_{s+}^t + \sum_{s \in \mathcal{S}} C_{s-}^t f_{s-}^t + \\ & \sum_{s \in \mathcal{S}} C_s^t V_s^t \end{aligned}$$

Power system constraints

The constraints of the electrical system represent the technical limits of the different elements that compose it, as well as the physical laws that govern it. For certain applications, the DC model is sufficient [Yang et al., 2019].



$$\underline{P}_g^t \leq P_g^t \leq \overline{P}_g^t \quad \forall g \in \mathcal{G}, \quad (6a)$$

$$-\overline{P}_l^t \leq P_l^t \leq \overline{P}_l^t \quad \forall l \in \mathcal{L}, \quad (6b)$$

$$P_l^t = B_{nm}(\theta_n - \theta_m) \quad \forall l = (n, m) \in \mathcal{L}, \quad (6c)$$

$$0 \leq P_d^t \leq \overline{P}_d^t \quad \forall d \in \mathcal{D}, \quad (6d)$$

$$-\overline{\theta}_n^t \leq \theta_m^t \leq \overline{\theta}_n^t \quad \forall n \in \mathcal{N}_P, \quad (6e)$$

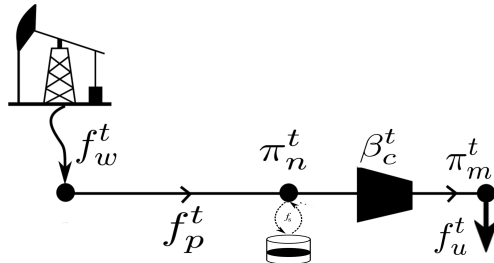
$$\sum_{\substack{l \in \mathcal{L}_{n+} \\ g=n}} P_l^t + P_g^t = \sum_{\substack{l \in \mathcal{L}_{n-} \\ d=n}} P_l^t + P_d^t \quad \forall n \in \mathcal{N}_P \quad (6f)$$

The second set of restrictions interconnects the natural gas and electric power systems through gas-fired power plants that generate electricity.

$$f_n^t = P_n^t \cdot \text{HR}_n, \quad \forall n \in \mathcal{N}_I, \quad (7)$$

Gas system constraints

This set of constraints ensures that wells, pipelines, nodal pressures, compressors, unsupplied demand and storage facilities operate within proper operating limits. [García-Marín et al., 2022].



$$\underline{f}_w^t \leq f_w^t \leq \overline{f}_w^t \quad \forall w \in \mathcal{W} \quad (8a)$$

$$-\overline{f}_p^t \leq f_p^t \leq \overline{f}_p^t \quad \forall p \in \mathcal{P} \quad (8b)$$

$$\underline{\pi}_n^t \leq \pi_n^t \leq \overline{\pi}_n^t \quad \forall n \in \mathcal{N}_f \quad (8c)$$

$$0 \leq f_u^t \leq \overline{f}_u^t \quad \forall u \in \mathcal{U} \quad (8d)$$

$$\sum_{m:(m,n) \in \mathcal{A}} f_m^t = \sum_{m':(n,m') \in \mathcal{A}} f_{m'}^t \quad \forall n \in \mathcal{N}_f \quad (8e)$$

$$\pi_m^t \leq \beta_c^t \pi_n^t \quad \forall c = (n, m) \in \mathcal{C} \quad (9a)$$

$$0 \leq f_{s+}^t \leq V_{0s} - \underline{V}_s \quad \forall s \in \mathcal{S} \quad (9b)$$

$$0 \leq f_{s-}^t \leq \overline{V}_s - V_{0s} \quad \forall s \in \mathcal{S} \quad (9c)$$

$$V_s^t = V_s^{t-1} + f_{s-}^t - f_{s+}^{t-1} \quad \forall s \in \mathcal{S} \quad (9d)$$

$$\text{sgn}(f_p^t)(f_p^t)^2 = K_{nm}((\pi_n^t)^2 - (\pi_m^t)^2) \quad \forall p = (n, m) \quad (9e)$$

Modeling the Weymouth equation as a nonconvex and discontinuous equality constraint presents significant challenges for optimization algorithms, leading to multiple local optima [Jiang et al., 2021].

Proposed complementarity-based approach

Complementarity constraints can be used to represent non-uniform or discontinuous operators, such as absolute value, sign, and min/max [Baumrucker et al., 2008]. The sign equation can be represented by an optimization problem whose constraints avoid the use of binary variables.

$$\mathcal{O}_\epsilon : \min_{y_p^t} -y_p^t f_p^t \quad (10a)$$

$$\text{s.t. } y_p^t (f_p^t)^2 = K_{nm} \left((\pi_n^t)^2 - (\pi_m^t)^2 \right) \quad (10b)$$

$$f_p^t = f_{p+}^t - f_{p-}^t \quad (10c)$$

$$-1 \leq y_p^t \leq 1 \quad (10d)$$

$$f_{p+}^t (y_p^t + 1) \leq \epsilon \quad (10e)$$

$$f_{p-}^t (1 - y_p^t) \leq \epsilon \quad (10f)$$

The regularized optimization model \mathcal{O}_ϵ offers several key properties that justify its use in tackling challenging MPCC problems [Ralph and Wright, 2004].

Databases

Each of the mentioned databases was selected based on its unique characteristics and the significant contributions it could make to the study.

	Topology	Connection points	Closed loops	Problem
Case 1	9-bus 8-system	1	1	Small system with one loop
Case 2	118-bus 48-system	9	7	Contains several interconnected loops
Case 3	96-bus 63-system	10	0	Fully radial but considers bidirectional flows.

Table 1: Databses used in the study

Experimental setup

In order to establish a baseline for comparison, two alternative methodologies were employed:

- Taylor series approximation [Fodstad et al., 2015].
- Second Order Cone Programming (SOC) [Schwele et al., 2019].

The objective function value for each of the mentioned databases was computed by solving the optimization problem using:

- The IPOPT [Wächter and Biegler, 2005] solver.
- The GEKKO [Beal et al., 2018] package.

Since understanding and quantifying the inherent errors introduced by any constraint approximation approach supports its real-world pertinence, the considered validation trades off the reached cost function and constraint error values.

$$WE_p^t = |f_p^t - \left(K_{nm} |(\pi_n^t)^2 - (\pi_m^t)^2| \right)^{1/2}|, \quad \forall p = (n, m) \in \mathcal{P} \quad (11)$$

Hence, WE_p^t metric explains the inherent sensitivity of tested approaches and validates the significance of their differences.

Results - Case 1

A Monte Carlo experiment estimates the cost function and Weymouth error distributions by solving the optimization problem for one single day one hundred times with uniformly sampled natural gas demands.

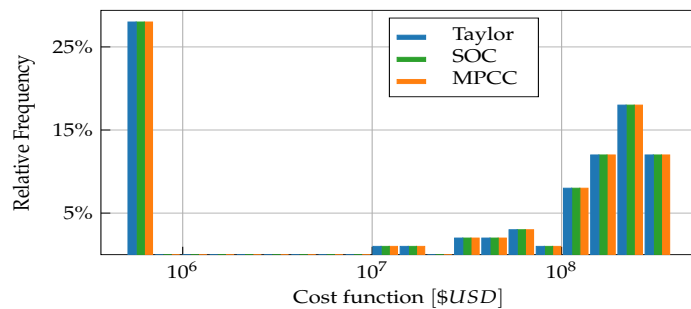


Figure 1: Cost function histogram attained for the Taylor, SOC, and MPCC Weymouth approximation approaches.

The boxplot examination reveals significantly lower approximation errors on the proposed complementarity constraints approach over key network arcs.

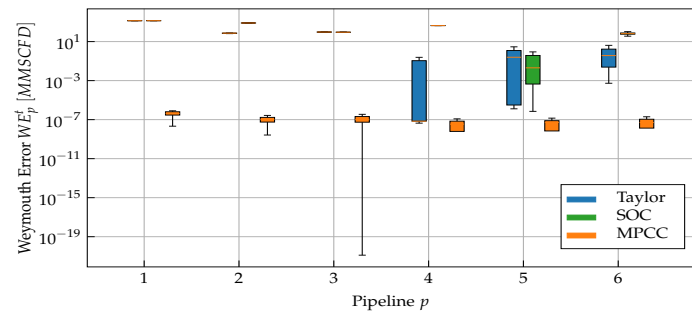


Figure 2: Boxplot of Weymouth error distribution for each pipeline in the 8/9 system attained by contrasted approximation approaches.

Results - Case 2

It is worth noting that both baselines yielded the same objective function values. The consistently positive relative difference indicates that the complementarity constraints formulation always yields larger cost values than Taylor and SOC for the 118/48 system.

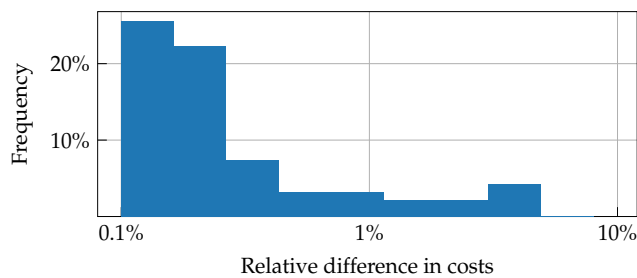


Figure 3: Histogram depicting the relative frequencies of cost differences obtained between MPCC and the other approaches in the 48-node 118-bus system.

Contrarily to cost function analysis, Weymouth approximation results reveal a significant error reduction of about seven orders of magnitude (from 10^1 to 10^{-6}) under the proposed complementarity constraints.

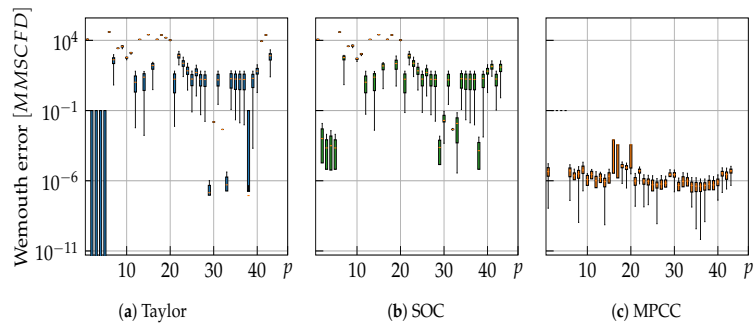


Figure 4: Weymouth approximation errors for each pipeline p reached by Taylor (left), SOC (center), and MPCC (right) approaches in the 118/48 system.

Results - Case 3

Instead of estimating the distributions of the objective function and Weymouth error as in cases 9/8 and 118/48, the 96/63 case validates the Weymouth approximations in an operation case of ten consecutive days ($|\mathcal{T}| = 10$) with randomly changing gas extraction costs.

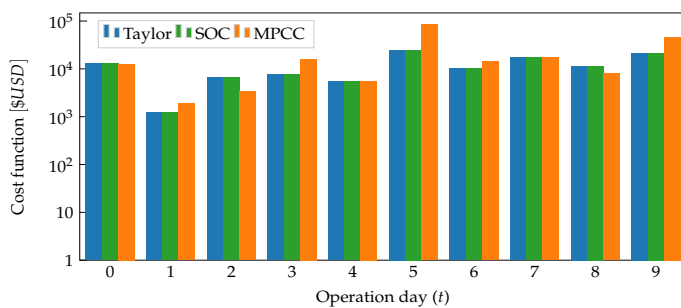


Figure 5: Daily operating cost obtained with each of the approaches in the 63-node 96-bus system.

Regarding the Weymouth approximation analysis, the figure presents the error distribution and its relationship with the gas flow and the scheduled day for Taylor, SOC, and MPCC.

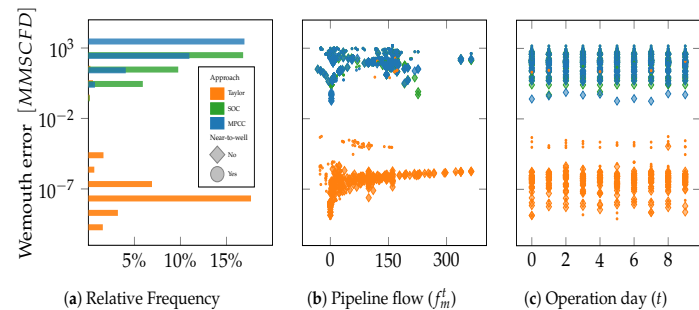


Figure 6: Errors in the Weymouth equation expressed in three different formats- general error, error per flow, and error per day.

Physics-Guided Neural Networks

Motivation:

- Traditional neural networks: fit data, ignore physics → risk of unrealistic predictions.
- In gas networks, physical constraints (mass balance, pressure-flow laws) are critical.

Physics-Informed Neural Networks (PINNs):

- Incorporate governing equations directly in the loss function.
- Penalize deviations from:
 - **Gas balance constraint** – nodal mass conservation.
 - **Weymouth equation** – relation between flow and pressure differences in pipelines.
- Acts as a *regularizer* for better generalization under uncertainty.

Methodology: Physics-Guided CensNet

Overall loss function:

$$\mathcal{J}(\Theta) = \mathcal{J}_{\text{data}} + \mathcal{J}_{\text{balance}} + \mathcal{J}_{\text{weymouth}}$$

Gas balance loss:

$$\mathcal{J}_{\text{balance}} = \mathbf{T} \cdot \hat{\mathbf{f}}_e - \mathbf{d} + \hat{\mathbf{f}}_n$$

- Enforces nodal inflow = outflow + demand.

Weymouth loss:

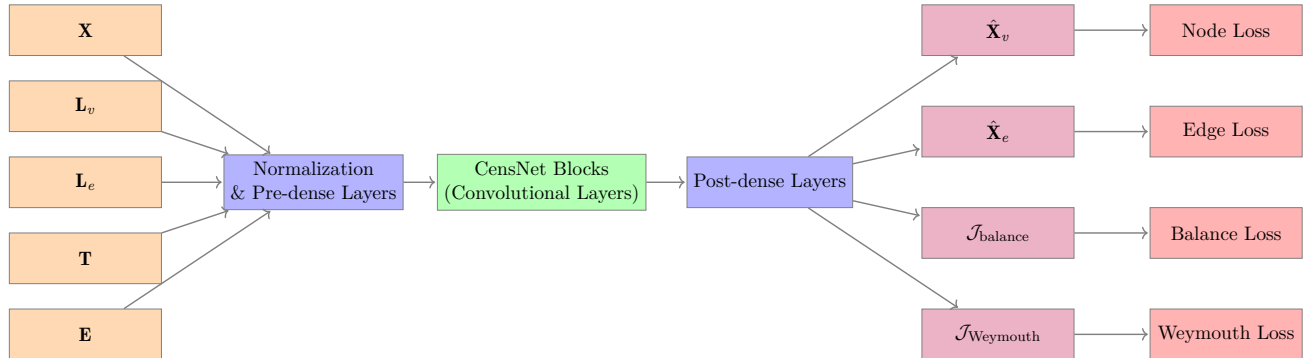
$$\mathcal{J}_{\text{weymouth}} = \mathbf{M}_{\mathcal{P}} \left(\hat{\mathbf{f}}_e^{\circ 2} - \mathbf{K} \circ \left(\mathbf{T} \cdot \hat{\boldsymbol{\pi}}^{\circ 2} \right) \right)$$

- Relates squared flows to squared pressure differences.
- Applies only to pipelines (not compressors).

Methodology: Physics-Guided CensNet

Implementation:

- Built on CensNet architecture from deterministic setup.
- Training data from nonlinear gas network optimization (MPCC).
- Noise (5%–25%) injected to emulate operating uncertainty.



Case Study I: 8-Node Network – Performance Comparison

Method	Node Error	Edge Error	Balance Error	Time (s)
CensNet (N)	0.00 ± 17.99	22.76 ± 15.43	-0.01 ± 17.45	0.86 ± 0.50
CensNet (N+E)	-0.11 ± 18.27	0.22 ± 21.65	-0.12 ± 1.70	0.85 ± 0.50
CensNet (N+E+B)	-0.02 ± 18.00	-0.02 ± 21.30	-0.03 ± 0.90	0.85 ± 0.50
CensNet (N+E+W)	-0.07 ± 17.56	2.60 ± 20.03	-0.07 ± 2.21	0.86 ± 0.50
CensNet (N+E+B+W)	0.05 ± 17.91	0.25 ± 21.14	0.05 ± 1.69	0.85 ± 0.50

Table 2: Performance of CensNet-based models vs. IPOPT benchmark.

- Using only node loss leads to accurate nodal flows but large errors in edge predictions.
- Adding edge loss (**N+E**) reduces edge error from 22.76 to 0.22 and improves global balance.
- Including balance loss (**N+E+B**) further minimizes balance error, achieving best overall consistency.
- Weymouth loss (**N+E+W**) introduces slight trade-offs, slightly increasing edge/balance errors but retaining nodal accuracy.
- All CensNet variants are over an order of magnitude faster than IPOPT, with **N+E+B** offering the best accuracy-speed compromise.

Stochastic Analysis: Methodology and results

Methodology:

- Kernel Density Estimate (KDE) fitted to training inputs.
- Synthetic samples generated and propagated through CensNet.
- Log-likelihoods compared for y_{sample} and \bar{y}_{train} .
- Kolmogorov–Smirnov (K–S) test used for distributional similarity.

Results:

- Log-likelihoods: $y_{\text{sample}} = -6.696 \times 10^6$, $\bar{y}_{\text{train}} = -6.657 \times 10^6$.
- K–S test: $p > 0.44$ across all alternatives.
- \Rightarrow Synthetic outputs statistically consistent with training outputs.

Negative Flows in Pipeline p_3

- Flow in p_3 consistently negative across scenarios and KDE samples.
- Caused by orientation assumption → optimizer adjusts direction.
- Operability unaffected, but p_3 supports cost minimization.

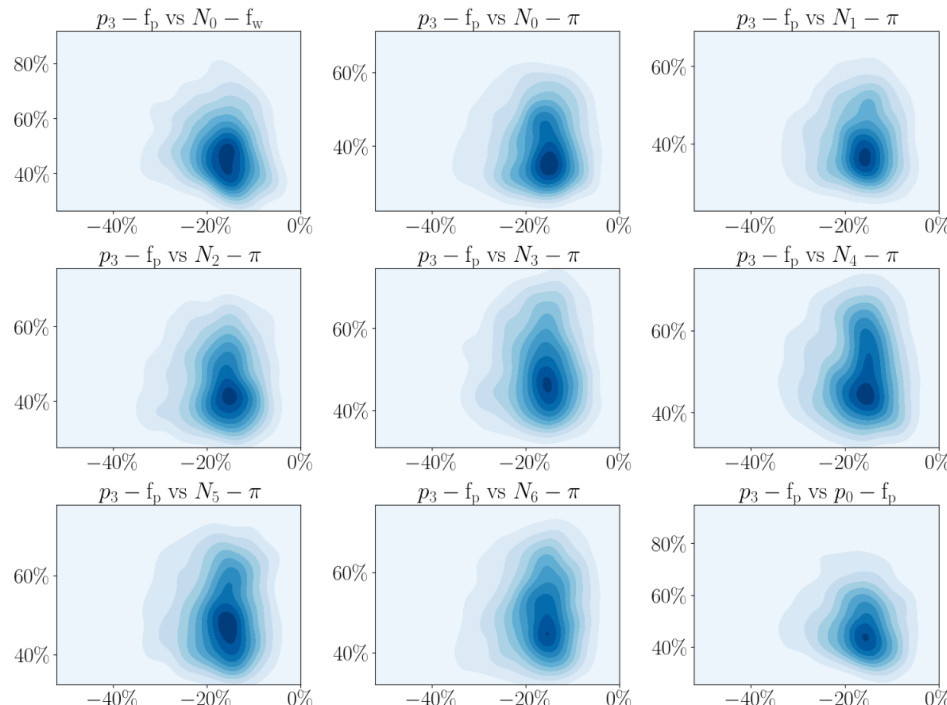


Figure 7: Joint PDFs showing negative p_3 flows.

Pressure Concentration in Mid-Range

- Nodal pressures cluster at 30–40% of normalized limits.
- Avoids extremes, ensuring reliable operation.
- Implies optimizer favors efficiency + stability.

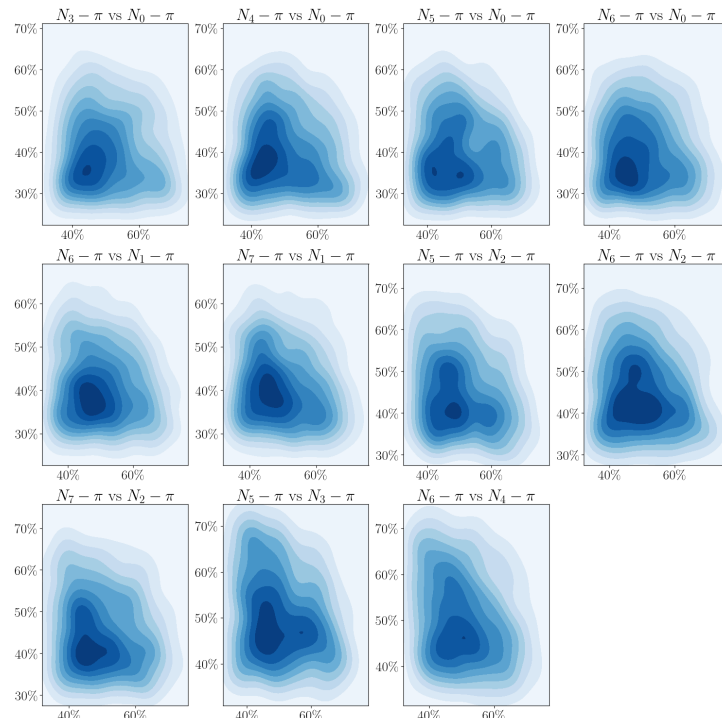


Figure 8: Pressures concentrate in mid-range (30–40%).

Stable Utilization of Pipeline p_4

- Despite wide dispersion in inputs, p_4 flow remains 20–40%.
- Reflects robustness: optimizer stabilizes this delivery path.
- Behavior consistently learned and reproduced in KDE samples.

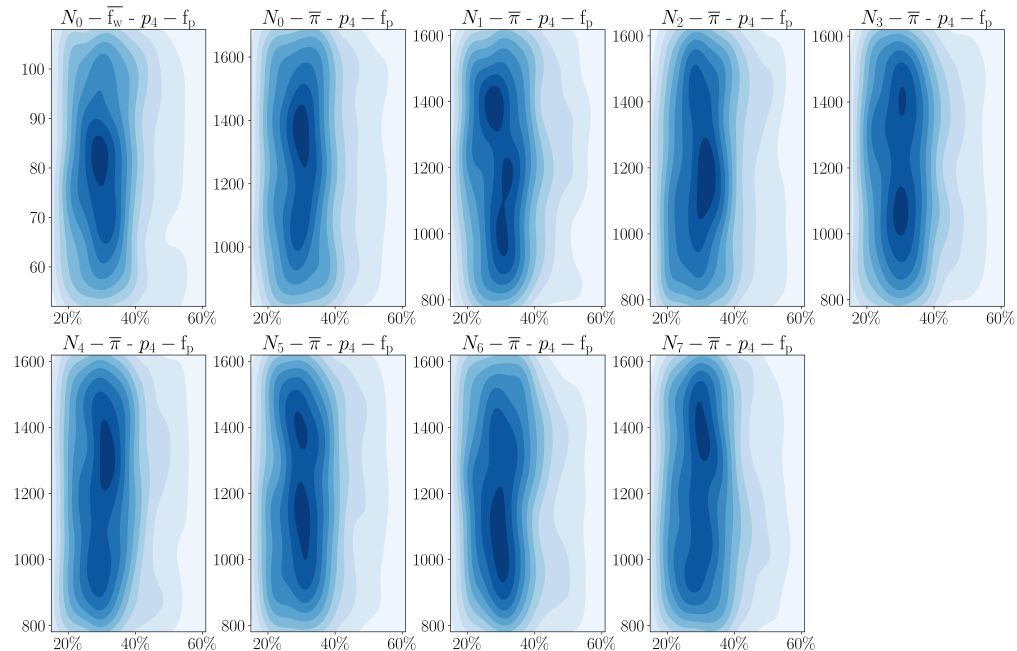


Figure 9: Optimization model: input variability vs. stable p_4 flow.

Linear Input–Output Relations

- Positive correlation: demand bounds (N_6, N_7) vs. p_4-p_7 flows.
- Negative correlation: N_7 demand bound vs. p_3 flow.
- Shows network internalized optimizer's allocation strategies.

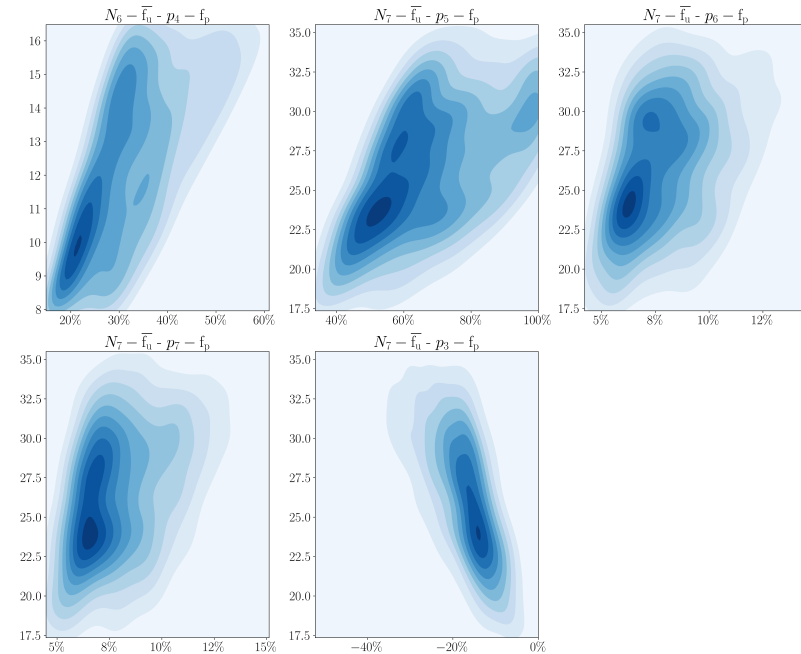


Figure 10: Optimization model: linear input–output patterns.

Conclusions

- **GNN-based prediction:** CensNet achieved accurate and scalable predictions for natural gas networks, with significant reductions in computation time compared to traditional optimization.
- **Optimization with MPCC:** Proposes a formulation to approximate Weymouth's restrictions, improving accuracy of pressure–flow representation and showing robustness in real-world scheduling tasks.
- **Stochastic modeling:** Physics-guided neural networks preserved structural dependencies and generalized reliably under uncertainty, validated through KDE sampling and K–S testing.
- **Overall:** Integrating physical constraints with GNNs yields efficient, accurate, and robust surrogates for optimization in natural gas systems.

Future Work

- Extend stochastic framework toward **full stochastic optimization** for gas–power coordination.
- Explore **physics-informed neural operators** to improve learning of nonlinear constraints (e.g., Weymouth).
- Incorporate **real operational data** from SCADA systems to validate scalability in live environments.
- Investigate **transfer learning across networks**, enabling models trained on one topology to adapt to others with minimal retraining.
- Apply developed methods to **decision-support tools** for dispatchers in interconnected energy systems.

References I



Baumrucker, B., Renfro, J., and Biegler, L. (2008).

Mpec problem formulations and solution strategies with chemical engineering applications.

Computers & Chemical Engineering, 32(12):2903–2913.



Beal, L. D. R., Hill, D. C., Martin, R. A., and Hedengren, J. D. (2018).

Gekko optimization suite.

Processes, 6(8).



Duan, J., Liu, F., and Yang, Y. (2022).

Optimal operation for integrated electricity and natural gas systems considering demand response uncertainties.

Applied Energy, 323:119455.

References II

-  Fodstad, M., Midthun, K. T., and Tomsgard, A. (2015).
Adding flexibility in a natural gas transportation network using interruptible transportation services.
European Journal of Operational Research, 243(2):647–657.
-  García-Marín, S., González-Vanegas, W., and Murillo-Sánchez, C. (2022).
Mpng: A matpower-based tool for optimal power and natural gas flow analyses.
IEEE Transactions on Power Systems, pages 1–9.

References III



Jiang, T., Yuan, C., Zhang, R., Bai, L., Li, X., Chen, H., and Li, G. (2021).

Exploiting flexibility of combined-cycle gas turbines in power system unit commitment with natural gas transmission constraints and reserve scheduling.

International Journal of Electrical Power & Energy Systems,
125:106460.



Pfetsch, M. E., Fügenschuh, A., Geißler, B., Geißler, N., Gollmer, R., Hiller, B., Humpola, J., Koch, T., Lehmann, T., Martin, A., and et al. (2014).

Validation of nominations in gas network optimization: Models, methods, and solutions.

Optimization Methods and Software, 30(1):15–53.

References IV

-  Promigas (2021).
Informe del sector gas natural 2021.
-  Ralph, D. and Wright, S. J. (2004).
Some properties of regularization and penalization schemes for
mpecs.
Optimization Methods and Software, 19(5):527–556.
-  Schwele, A., Ordoudis, C., Kazempour, J., and Pinson, P. (2019).
Coordination of power and natural gas systems: Convexification
approaches for linepack modeling.
In *2019 IEEE Milan PowerTech*, pages 1–6.

References V

-  Sharifi, V., Abdollahi, A., Rashidinejad, M., Heydarian-Forushani, E., and Alhelou, H. H. (2022).
Integrated electricity and natural gas demand response in flexibility-based generation maintenance scheduling.
IEEE Access, 10:76021–76030.
-  Wächter, A. and Biegler, L. T. (2005).
On the implementation of an interior-point filter line-search algorithm for large-scale nonlinear programming.
Mathematical Programming, 106(1):25–57.
-  Yang, Z., Xie, K., Yu, J., Zhong, H., Zhang, N., and Xia, Q. (2019).
A general formulation of linear power flow models: Basic theory and error analysis.
IEEE Transactions on Power Systems, 34(2):1315–1324.